Chemical Poisoning of Ni/MgO Catalyst by Alkali Carbonate Vapor in the Steam Reforming Reaction of DIR-MCFC

Hyeung-Dae Moon, Tae-Hoon Lim,† and Ho-In Lee*

School of Chemical Engineering, Seoul National University, Seoul 151-742, Korea
†Battery and Fuel Cell Research Center, Korea Institute of Science and Technology, P.O. Box 131, Cheongryang, Seoul 130-650, Korea
Received October 9, 1999

Chemical poisoning of Ni/MgO catalyst was induced by hot alkali carbonate vapor in molten carbonate fuel cell (MCFC), and the poisoned (or contaminated) catalyst was characterized by TPR/TPO, FTIR, and XRD analysis. Carbonate electrolytes such as K and Li were transferred to the catalyst during DIR-MCFC operation at 650 °C. The deposition of alkali species on the catalyst consequently led to physical blocking on catalytic active sites and structural deformation by chemical poisoning. TPR/TPO analysis indicated that K species enhanced the reducibility of NiO thin film over Ni as co-catalyst, and Li species lessened the reducibility of metallic Ni by chemical reaction with MgO. FTIR analysis of the poisoned catalyst did not exhibit the characteristic $\upsilon_1(D_{3h})$ peaks (1055 cm^{-1}, 1085 cm^{-1}) for pure crystalline carbonates, instead a new peak (1120 cm^{-1}) was observed proportionally with deformed alkali carbonates. From XRD analysis, the oxidation of metallic Ni into $Ni_xMg_{1-x}O$ was confirmed by the peak shift of MgO with shrinking of Ni particles. Conclusively, hot alkali species induced both chemical poisoning and physical deposition on Ni/MgO catalyst in DIR-MCFC at 650 °C.

Introduction

Methane is a common fuel utilized in a molten carbonate fuel cell of direct internal reforming type, in which steam reforming reaction of methane ($CH_4 + H_2O \rightarrow CO + 3H_2$) occurs simultaneously with the electrochemical oxidation of hydrogen ($H_2 + CO_3^{2-} \rightarrow H_2O + CO_2 + 2e^-$) in the anode component.[1,2] The catalyst inside the molten carbonate fuel cell should be active for the steam reforming of hydrocarbons, especially methane abundant in natural gas, at the operating temperature of MCFC.[3] However, such reforming catalysts gradually lose their activity due to chemical poisoning by alkali metal carbonates (or alkali metal hydroxides) generated from electrolyte components such as K_2CO_3 and Li_2CO_3.[4,5] Despite that basic oxides generally have poor reactivity toward alkali species,[6] lithium exhibits some affinity for MgO[7] and NiO[8,9] lattices, probably due to its similar ionic radius with Mg^{2+} and Ni^{2+}. Small amounts of Li^+ can be incorporated into MgO lattice by creating electron holes,[7] whereas Li^+ and NiO form $Li_xNi_{1-x}O$ solid solution in a wide composition range, $0 < x < 0.6$.

In recent days, Ni/MgO catalyst has been investigated in some details by many researchers. In DIR-MCFC operation for 860 hrs, Cavallaro *et al.*[10] observed that alkali species deactivated the catalyst by pore blocking mechanism, *i.e.*, KOH glassy layer blocked the active sites by covering the whole external surface of the catalyst. Kitabayashi has shown that Ni amounts was increased in Ni/MgO catalyst by the contamination of K_2CO_3 in spite of the diminishment of steam reforming activity. Rostrup-Nielson[11] has shown that alkali metals did not affect the sintering of Ni crystallites under steam reforming conditions, but rather induced reconstruction (faceting) of less active nickel [111] surface. There is still controversy on the mechanism of alkali poisoning on reforming catalyst in DIR-MCFC operation. In this research, chemical poisoning by hot alkali species was investigated by the microscopic analysis of Ni/MgO catalyst in unit cell after MCFC operation for 72 hrs.

Experimental Section

Single cell of DIR-MCFC was composed of cell body (made of stainless steel), anode, cathode, alkali carbonate electrolytes (K_2CO_3; 38 mol% + Li_2CO_3; 62 mol%), electrolyte matrix, current collector, and reforming catalyst. The dimension of each electrode was 5 cm × 5 cm. The operating temperature and atmosphere were adjusted gradually up to 650 °C for the crack-protection and activation of each cell component. The reforming catalyst was prepared as commercial cylindrical pellet and located inside the gas channel where hydrocarbons were converted into H_2 by steam reforming reaction.

After 72 hrs' operation, DIR-MCFC single cell was quenched under hydrogen-rich flow condition in order to prevent alkali contamination, and the catalysts were sampled at different position of the cell. Fresh catalyst was designated by FC, and deactivated catalysts sampled at different positions (inlet, middle, outlet) of the gas channel were designated as UC(1/3), UC(2/3), and UC(3/3), respectively.

The characteristics of the catalyst were analyzed by various microscopic instruments such as SEM, TPR/TPO, FTIR, and XRD. Elemental analysis of alkali species was performed by ICP device. The dispersion of Ni element over MgO support was measured by H_2-chemisorption. Reducibility of Ni on the catalyst was examined by TPR/TPO (Temperature Programmed Reduction/Oxidation) method.

FTIR and XRD analysis were performed to detect the physico-chemical changes of the catalyst before and after experiment.

Results and Discussion

Elemental Analysis. In our previous study for the physical poisoning by hot alkali carbonate vapor,[12] it was revealed that potassium (K) and lithium (Li), the components of carbonate electrolytes, were transferred to the catalyst during DIR-MCFC operation at 650 °C. From elemental analysis by ICP, the amount of K species was increased in the order of UC(2/3); 1.53 wt%, UC(3/3); 4.97 wt%, UC(1/3); 8.67 wt%, while Li species were increased in the order of UC(2/3); 0.85 wt%, UC(1/3); 1.72 wt%, UC(3/3); 2.45 wt%.

SEM Image Analysis. The surface images of the catalysts FC, UC(2/3), and FC-A were shown in Figure 1. FC-A was the catalyst contaminated by carbonate vapor in the anode chamber during non-flow quenching operation of DIR-MCFC. Alkali species transferred to FC-A had not sufficient time and enough energy to react with Ni/MgO. The fresh catalyst FC had rougher and cleaner surface than the contaminated catalysts UC(2/3) and FC-A.[10,11] The difference between UC(2/3) and FC-A catalysts was the crystallization degree of contaminants. Alkali species in the catalyst UC(2/3) was non-crystalline glassy material, while the contaminants on the catalyst FC-A were crystalline alkali species. This suggested that alkali carbonates deposited on Ni/MgO catalyst could be transformed from crystalline alkali carbonates (or alkali hydroxides) to glassy material at high temperature, and the reduction of catalytic sites by alkali contamination was a main factor in the deactivation of DIR-MCFC.

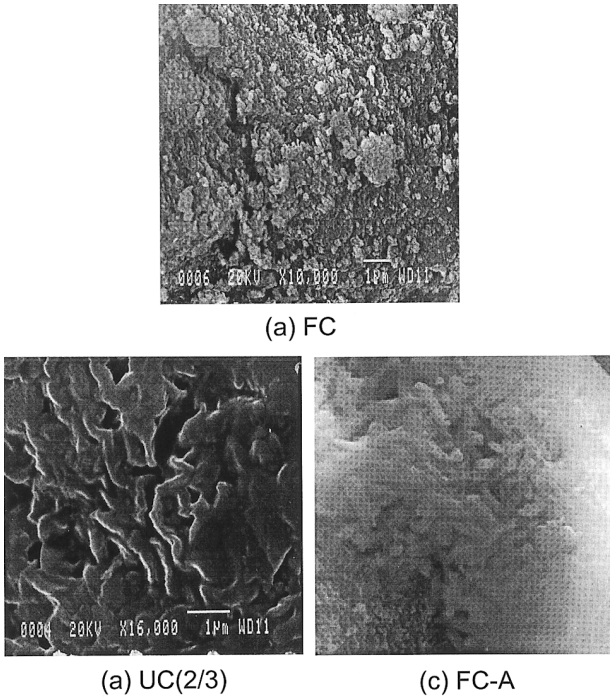

Figure 1. SEM photographs of catalysts (a) FC, (b) UC(2/3), and (c) FC-A.

Temperature Programmed Reduction and Oxidation (TPR/TPO). Reducibility of Ni elements on the catalyst was examined by temperature programmed reduction/oxidation (TPR/TPO) method. TPR/TPO analysis was carried out in a differential micro reactor at following conditions: heating rate; 10 K/min, catalyst weight; 20 mg Ni, flow rate; 20 mL/min, flow gas composition; 7.5% H_2 diluted by N_2 (in TPR experiment) and 5.0% O_2 diluted by He (in TPO experiment). H_2 and O_2 concentration were measured by a gas chromatography equipped with TCD (thermal conductivity detector). Before conducting TPO experiment, all the catalysts were sufficiently reduced at 800 °C and quenched under hydrogen-rich flow.

TPR: Figure 2 exhibited the reduction peak for NiO passivation layer over metallic Ni surface. For the catalysts FC, UC(1/3), UC(2/3), and UC(3/3), maximum peaks were observed at 292 °C, 236 °C, 265 °C, and 260 °C, respectively. As more alkali metals were incorporated into the catalyst, NiO reduction peak was shifted to lower temperature in the order of UC(1/3), UC(2/3), and UC(3/3). This indicated that alkali species induced not only physical blocking of the catalytic sites but also the modification of chemical properties of the catalyst. In many industrial processes (such as hydrogenation, steam reforming, and methanation), small amounts (0.5-1.0 wt%) of alkali ions impregnated on metal-supported catalysts made a substantial influence on the catalytic activities and lifetimes.[13] Especially, K has been well known as a catalyst promoter in eliminating carbon deposits.[14] Quantum mechanical calculations for the Nickel[111] surface[15] elucidated that adsorbed potassium atoms had a significant impact on the electronic properties of metallic Ni. In general, alkali metals increase the electron density of nearby metallic element and enhance the reducibility of the element. Hence, electron donating effect was considered as the main cause for the shift of NiO peak to lower temperature. For the catalyst FC, the peak ranged from 300 °C to 400

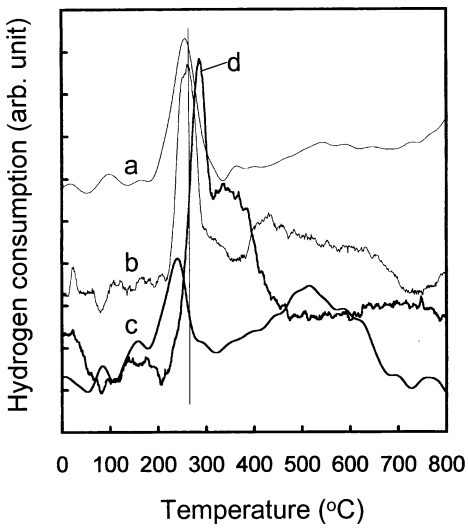

Figure 2. TPR profiles of various catalysts (a) UC(1/3), (b) UC(2/3), (c) UC(3/3), and (d) FC.

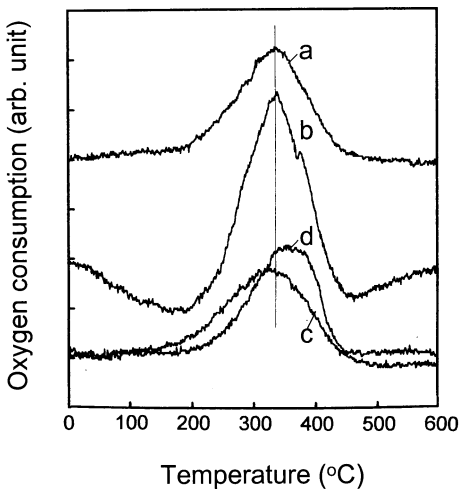

Figure 3. TPO profiles of various catalysts (a) UC(1/3), (b) UC(2/3), (c) UC(3/3), and (d) FC.

°C was assigned to bulk NiO reduction peak at the initial state.

TPO: Figure 3 showed the oxidation peak of metallic Ni. The fresh catalyst FC exhibited an asymmetric peak ranged from 330 °C to 390 °C, and the contaminated catalysts UC(1/3), UC(2/3), and UC(3/3) exhibited symmetric peaks of lower temperature. This indicated that oxidizability of metallic Ni in the contaminated catalyst was increased by the poisoning effect of hot alkali vapor. In the consideration of co-catalytic function of K, the decrease of reducibility of Ni was not caused by K species but by Li species.[10,11] For instance, Li^+ ion could affect the physico-chemical properties (such as basic strength and electronic conductivity) of MgO even with very small amounts.[16,17] Cosimo *et al.*[16] studied catalytic promotion effect on vapor phase aldol condensation over MgO catalyst with 0.7-1.0 wt% alkali (Li, Na, K, Cs) and alkali earth (Ca, Sr and Ba) metal ions. High strength of basic property in Li/MgO was induced by replacing Mg^{2+} with Li^+ in the MgO lattice. They also claimed that the replacement of metallic ions resulted in strained MgO bond and Li^+O^- formation, consequently leading to generation of strong basic sites. Conclusively, the modification of MgO lattice by Li ion[16,17] influenced the oxidization property of metallic Ni. K species made an effect on the oxidizability of NiO thin film as co-catalyst, and Li species changed the properties of bulk Ni by chemical reaction with MgO.

FTIR Analysis. IR spectra were registered on FTIR spectrometer with a spectral resolution of 4 cm^{-1}. The fundamental vibration spectra of carbonate ion was summarized in Table 1.[18] The free carbonate ion (D_{3h} symmetry) represented three IR active bands: υ_3(E) of asymmetric υ(CO) vibration; 1415 cm^{-1}, $\upsilon_2(A_2')$ out of plane $\pi(CO_3)$ deformation; 879 cm^{-1}, ν_4(E) in plane $\delta(CO_3)$ deformation; 680 cm^{-1}. In the adsorbed state, the symmetry was lowered by forming two υ_3 (CO) bands around 1415 cm^{-1}.[18] Due to the loss of D_{3h} symmetry, degenerate $\Delta\upsilon_3$ vibration was splitted into two bands. $\Delta\upsilon_3$ splitting was supposed to represent the

Table 1. Fundamental Vibration Spectrum of Carbonate Ions (D_{3h})[16]

Assignment	Frequency (cm^{-1})
Asymmetric ν (CO) stretch, ν_3(E)	1415
Symmetric ν (CO) stretch, $\nu_1(A_1')$	1063
(IR active only at loss of symmetry)	
Out of plane $\pi(CO_3)$ deformation, $\nu_2(A_2')$	879
In plane $\delta(CO_3)$ deformation, ν_4(E)	680

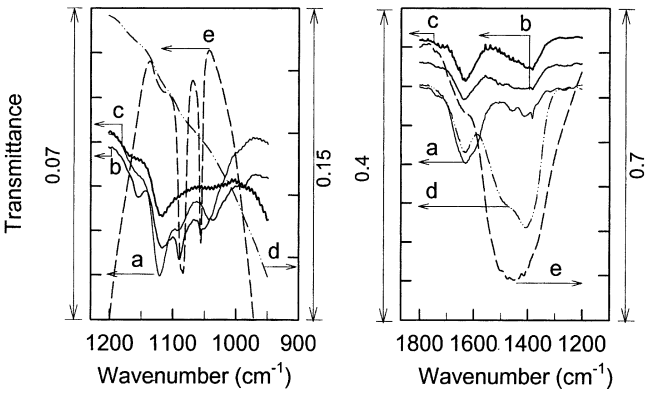

Figure 4. FTIR spectra of various catalysts (950-1200 cm^{-1} and 1200-1800 cm^{-1}) (a) UC(1/3), (b) UC(2/3), (c), UC(3/3), (d) FC, and (e) FC-A.

structural characteristics of the species, *i.e.*, Wavenumbers of 100, 300 and 400 cm^{-1} represented for monodentate, bidentate, and bridged species, respectively.[18,19] In addition, the loss of D_{3h} symmetry due to CO_2 adsorption slightly activated υ_1 band (close to 1063 cm^{-1}) to infrared.[18]

Figure 4 exhibited FTIR spectra in the range of 950-1800 cm^{-1} for the catalysts FC, UC(1/3), UC(2/3), UC(3/3) and FC-A. For the fresh catalyst FC, there was no trace of alkali carbonates. For the catalyst FC-A, $\upsilon_1(A_1')$ peaks for pure carbonate ion[18] and bicarbonate ion[18] were observed at 1055 cm^{-1} and 1085 cm^{-1}, respectively. At low temperature (< 650 °C), alkali carbonates maintained its characteristics as pure alkali carbonates. For the catalysts UC(1/3), UC(2/3), and UC(3/3) at 650 °C, however, the characteristic peak of pure alkali carbonate or bicarbonate was not detected, but a peak near 1120 cm^{-1} was observed proportionally with alkali contents. The new peak was assigned to deformed alkali carbonates. Most of alkali species in the catalyst at 650 °C lost their characteristic properties by interaction with Ni/MgO elements. The catalyst UC(2/3) with lowest alkali carbonates exhibited highest residual pure carbonates among the contaminated catalysts. In summary, the catalysts UC(1/3) and UC(3/3) were deactivated more severely than the catalyst UC(2/3), and the catalytic activity for steam reforming reaction was increased in the order of UC(3/3), UC(1/3), and UC(2/3).[12]

For the catalyst FC-A, the peak observed near 1415 cm^{-1} was confirmed as pure alkali carbonates.[18] Asymmetric (CO) stretching peak, υ_3(E), was observed at 1415 cm^{-1}. This peak must be induced by CO_2 adsorption because FC contained no trace of alkali carbonates. On the contrary, the υ_3(E) peak was hardly detected in the catalysts UC(1/3),

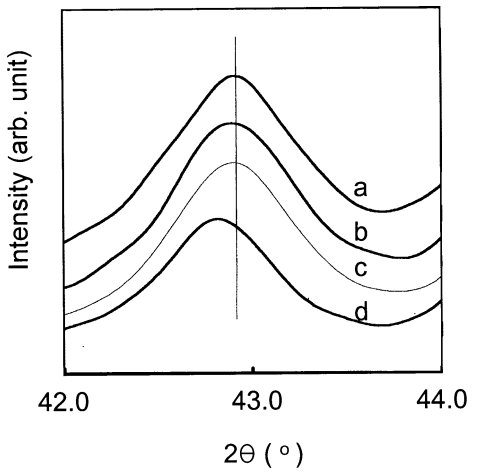

Figure 5. XRD patterns of various catalysts (2θ = 42.0-44.0°) (a) UC(1/3), (b) UC(2/3), (c) UC(3/3), and (d) FC.

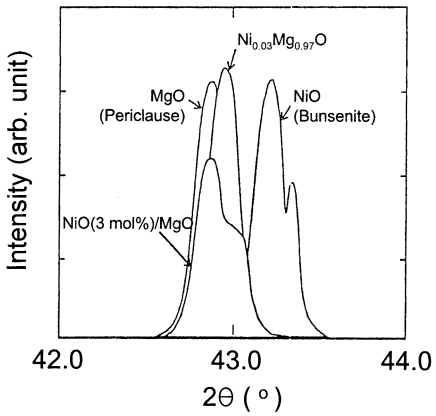

Figure 6. XRD patterns of Ni-Mg-O catalysts (2θ = 42.0-44.0 °).[18]

UC(2/3), and UC(3/3), indicating that the alkali species did not exist as pure carbonates in the contaminated catalysts. CO_2 seemed to adsorb as the state of CO and O splitted by strong basic site, Li^+O^-.[16] Except for Li^+O^- formation, the contaminated catalysts might have many strong basic sites responsible for CO adsorption. For example, the structural defects[20] like edges (or steps) with low coordination number could be generated during DIR-MCFC operation under high temperature and reduction atmosphere, and these defects could act as another strong basic site.[20,21] The peak near 1630 cm^{-1} for the contaminated catalysts was closely related to deformed carbonates because the peak intensity was increased in the order of UC(2/3), UC(3/3), and UC(1/3) with rising alkali amounts. From FTIR analysis, alkali carbonates transferred to Ni/MgO catalyst did not sustain its own pure carbonate structures at 650 °C, and CO_2 adsorption on MgO support was significantly influenced by deformed alkali species.

XRD Analysis. The crystalline phases of the catalyst was analysed by X-ray powder diffractometry (18 kW) using CuKα_1 radiation. Measurements were performed in a 2θ interval from 20 to 70 with a step of 0.02 deg. The mean particle size of Ni was calculated from the line broadening of Ni[200] peak (2θ = 51.7°) by Scherrer equation. Instrumental line width was compensated by Ni[200] line broadening measurement of Ni foil.

XRD analysis was performed to elucidate the effect of hot alkali species on MgO support. Figure 5 presented XRD patterns for the catalysts FC, UC(1/3), UC(2/3), and UC(3/3). The peak at 42.8° was assigned to MgO[22] or NiO.[23] The characteristic peak for NiO and MgO had nearby position with each other because the two materials had the same rock salt structure and similar ionic radius (e.g., Mg^{2+}; 72 pm, Ni^{2+}; 69 pm). There was no abrupt structural changes in the catalysts FC, UC(1/3), UC(2/3) and UC(3/3). However, all MgO peaks for the contaminated catalysts were shifted to higher degree than that of the fresh catalyst. The shift of MgO peak also indicated the deformation of MgO support by hot alkali species during fuel cell operation at 650 °C. In addition, the peak shift to higher degree implied the shrinkage or buckling of MgO lattice by chemical reaction between MgO and alkali carbonates, especially Li ion.[15,16]

Another possibility for the peak shift could be suggested as the formation of $Ni_xMg_{1-x}O$ solid solution by the reaction of MgO with Ni as shown in Figure 6. Yamazaki *et al.*[24] studied XRD peak shift induced by the formation of $Ni_xMg_{1-x}O$ solid solution, and ascertained that MgO peak was shifted to higher degree with rising Ni contents of $Ni_xMg_{1-x}O$. From XRD analysis by Scherrer equation, average particle size of Ni was calculated as 1.83 nm, 1.72 nm, 0.79 nm, and 0.73 nm, respectively, for the catalysts FC, UC(1/3), UC(2/3), and UC(3/3). It was concluded that hot alkali species deformed the properties of Ni/MgO catalyst and induced partial oxidation of metallic Ni into $Ni_xMg_{1-x}O$ with shrinking of Ni particles.

Conclusions

Chemical poisoning of Ni/MgO catalyst by hot alkali species was distinctly observed in DIR-MCFC at 650 °C, and the poisoned catalyst was characterized by ICP, TPR/TPO, FTIR and XRD analysis, in terms of property changes of Ni and MgO. The deactivation of the reforming catalyst in DIR-MCFC was mainly attributed by physical deposition and chemical poisoning of alkali carbonates. Alkali species deposited on Ni/MgO catalyst activated the oxidation of metallic Ni into $Ni_xMg_{1-x}O$ and deformed the properties of alkali carbonates, MgO, NiO film over Ni, and metallic Ni. The oxidation resistance of metallic Ni was diminished by alkali contents, but the reducibility of NiO thin film was enhanced. In summary, hot alkali carbonates transferred to Ni/MgO catalyst reacted with MgO, and then metallic Ni was oxidized into $Ni_xMg_{1-x}O$. The reducibility of NiO was increased by K species, whereas the reducibility of Ni was decreased by Li species.

Acknowledgments. This work was financially supported by R&D Management Center for Energy and Resources (RaCER), The Korea Energy Management Corporation. The authors are grateful to professor Sangwha Lee in Kyungwon University for his help in the preparation of the manuscript.

References

1. Appleby, A. J.; Foulkes, F. R. *Fuel Cell Handbook*; Van Nostrand Reinhold: 1989.
2. Shores, D.; Maru, H.; Uchida, I.; Selman, J. R. *Proceedings of the Third International Symposium on Carbonate Fuel Cell Technology*; The Electrochemical Society, Inc.: 1993.
3. Berger, R. J.; Doesburg, E. B. M.; van Ommen, J. G.; Ross, J. R. H. *Appl. Catalysis A: Gen*. **1996**, *143*, 343.
4. Selman, R. J. *Energy*(Oxford) **1986**, *11*, 153.
5. Tarjanyi, M.; Paetch, L.; Bernard, R.; Ghezel-Ayagih, H. *Reprints of Fuel Cell Seminar*; Tucson, AZ, 1985; p 177.
6. Moral, P.; Praliaud, H.; Martin, G. A. *React. Kinet. Catal. Lett*. **1987**, *34*, 1.
7. Catlow, C. R. A.; Jackson, R. A.; Thomas, J. M. *J. Phys. Chem*. **1990**, *94*, 7889.
8. Bielanski, A.; Deren, J.; Haber, J.; Sloczynski, J. *Trans. Faraday Soc.* **1966**, *58*, 166.
9. Cochran, S. J.; Larkins, F. P. *Aust. J. Chem.* **1985**, *38*, 1293.
10. Cavallaro, S.; Freni, S.; Cannistraci, R.; Aquino, M.; Giordano, N. *Int. J. Hydrogen Energy* **1992**, *17*(3), 181.
11. Rostrup-Nielsen, R. J.; Christiansen, L. J. *App. Catalysis A* **1995**, *126*, 381.
12. Moon, H.-D.; Kim, J.-H.; Ha, H. Y.; Lim, T.-H.; Hong, S.-A.; Lee, H.-I. *J. Korean Ind. Eng. Chem.* accepted.
13. Demicheli, M. C.; Duprez, D.; Barbier, J.; Ferretti, O. A.; Ponzi, E. N. *J. Catal*. **1994**, *145*, 437.
14. Rostrup-Nielson, R. J. "Catalytic Steam Reforming"; Anderson, J. R., Bourdart, M., Eds.; *Catalysis, Science and Technology*; Springer: Berlin, 1984; Vol. 5, pp 1-120.
15. Simon, D.; Bigot, E. *Surf. Sci*. **1994**, *306*, 459.
16. Di Cosimo, J. I.; Diez, V. K.; Apesteguia, C. R. *Appl. Catal.* **1996**, *137*, 149.
17. Norby, T.; Andersen, A. G. *Appl. Catal.* **1991**, *71*, 89.
18. Lavalley, J. C. *Catal. Today* **1996**, *27*, 377.
19. Busca, G.; Lorenzelli, V. *Mater. Chem*. **1982**, *7*, 89.
20. Guglielminotti, E.; Coluccia, S.; Garrone, E.; Cerruti, L.; Zecchina, A. *J. Chem. Soc., Farad. Trans. 1* **1981**, *77*, 1063.
21. Tsyganenko, A. A.; Lamotte, J.; Gallas, J. P.; Lavalley, J. C. *J. Phys. Chem*. **1984**, *23*, 177.
22. Parra Soto, J. B. *J. Catal.* **1994**, *148*, 403.
23. Lamber, R.; Ekloff, G. S. *J. Catal*. **1994**, *146*, 601.
24. Yamazaki, O.; Tomishige, K.; Fujimoto, K. *Appl. Catalysis A: Gen.* **1996**, *136*, 49.